agriculture

MDPI

Article

Overexpression of *CsGSH2* Alleviates Propamocarb Residues and Phytotoxicity in Cucumber by Enhancing Antioxidant and Glutathione Detoxification Properties

Shengnan Li [1], Zedong Wu [1], Chunhong Liu [2], Lianxue Fan [2], Yongheng He [1], Ke Lu [1], Dajun Liu [1,*] and Guojun Feng [1,*]

[1] College of Advanced Agriculture and Ecological Environment, Heilongjiang University, Harbin 150080, China
[2] College of Horticulture and Landscape Architecture, Northeast Agricultural University, Harbin 150030, China
* Correspondence: 2016003@hlju.edu.cn (D.L.); 2016002@hlju.edu.cn (G.F.)

Abstract: Propamocarb is a pesticide widely used to control cucumber downy mildew. The overuse of propamocarb has resulted in residues and phytotoxicity. However, the detoxification and metabolic process of propamocarb have not been documented well. Our previous work showed differences in the propamocarb residues among the different genotypes of cucumber and their regulation by multiple genes. Based on the already reported data on gene expression profiles under propamocarb treatment, we identified the glutathione pathway, including six different genes (*Csa4M303130*, *Csa3M133380*, *Csa5M409710*, *Csa7M395820*, *Csa3M597320*, and *Csa1M571280*), involved in propamocarb detoxification. The qPCR analysis showed that *Csa1M571280* (*CsGSH2*) was most significantly and differentially expressed at 48 h after propamocarb spray in the cucumber varieties Y3F604 (low propamocarb residues) and M729 (high propamocarb residues). In Y3F604, *CsGSH2* expression increased from 6 to 48 h after spraying propamocarb, and the expression was positively correlated with propamocarb residues, whereas M729 showed no significant difference in *CsGSH2* expression. Therefore, we presumed *CsGSH2* as a key gene in managing propamocarb residues. Gene functional analysis showed that propamocarb residues decreased in *CsGSH2*-overexpressing plants and increased in *CsGSH2*-antisense plants. Overexpression of *CsGSH2* enhanced glutathione (GSH) accumulation and glutathione S-transferase (GST), glutathione reductase (GR), and glutathione peroxidase (GPX) activities, probably for propamocarb detoxification. The activity of antioxidant enzymes (SOD, POD, CAT, and APX) increased to maintain a high antioxidant capacity in *CsGSH2*-overexpressing plants. The superoxide (O^{2-}), hydrogen peroxide (H_2O_2), and malondialdehyde (MDA) levels decreased in *CsGSH2*-overexpressing plants, promoting the antioxidant system composed of ascorbic acid and glutathione (AsA-GSH). Thus, we conclude that *CsGSH2* alleviates propamocarb residues and phytotoxicity by enhancing cucumber's antioxidant and glutathione detoxification potential.

Keywords: cucumber; propamocarb; antioxidant; glutathione; detoxification

Citation: Li, S.; Wu, Z.; Liu, C.; Fan, L.; He, Y.; Lu, K.; Liu, D.; Feng, G. Overexpression of *CsGSH2* Alleviates Propamocarb Residues and Phytotoxicity in Cucumber by Enhancing Antioxidant and Glutathione Detoxification Properties. *Agriculture* **2022**, *12*, 1528. https://doi.org/10.3390/agriculture12101528

Academic Editor: Eduardo Rosa

Received: 12 July 2022
Accepted: 20 September 2022
Published: 23 September 2022

1. Introduction

Propamocarb is a highly effective bactericide used to control cucumber downy mildew. It belongs to the carbamate pesticide family and restrains fungal growth by suppressing the phosphoric acid and fatty acid synthesis pathways [1,2]. However, it easily results in residues in cucumber leaves, fruits, and other tissues. Residues and phytotoxicity due to propamocarb are unavoidable and threaten food safety. The propamocarb residues settle in the soil, river, and sea, resulting in environmental pollution. These residues enter the food chain and cause a potential threat to human health [3]. Meanwhile, an excessive use of propamocarb results in yellow speckles on leaves and necrosis of the shoot apical meristem [4,5]. However, little is known about propamocarb degradation and metabolism in cucumbers.

The overuse of propamocarb induces high levels of reactive oxygen species (ROS), such as superoxide (O_2^-) and hydrogen peroxide (H_2O_2) [4]. Typically, plants depend on their antioxidant system, including enzymatic and nonenzymatic compounds, to protect against ROS damage [6]. In the antioxidant enzymatic system, superoxide dismutase (SOD), peroxidase (POD), catalase (CAT), ascorbate peroxidase (APX), and glutathione peroxidase (GPX) are essential for ROS scavenging [7]. In the nonenzymatic system, the ascorbate–glutathione (AsA-GSH) cycle plays a crucial role in ROS scavenging and detoxification [8]. Glutathione (GSH) forms a redox cycle with AsA to consume H_2O_2 and act as a recycled intermediate for H_2O_2 reduction [9]. APX consumes H_2O_2 and oxidizes AsA to monodehydroascorbate (MDHA), which gets reduced to AsA. Then, dehydroascorbate reductase (DHAR) oxidizes GSH to glutathione disulfide (GSSG), and DHA is reduced to AsA. Meanwhile, glutathione reductase (GR) restores GSSG as GSH with NAD(P)H [10]. Therefore, enhancing the antioxidant systems for ROS scavenging is crucial in protecting against propamocarb stress and phytotoxicity.

Studies have shown that the exposure to light and application of brassinosteroids (BRs) and melatonin (Mel) alleviated pesticide phytotoxicity in plants [11–13]. However, eliminating pesticide residues from the internal plant tissues is particularly difficult, regardless of the approach. Plants protect themselves from pesticides via complex mechanisms including oxidation, reduction, hydrolysis, dehalogenation, and conjugation. In plants, herbicides and pesticides become oxidized into water-soluble metabolites with high polarity by the hydrolytic action of cytochrome P450s and POD and reactions catalyzed by GST and glycosyltransferases, which can convert toxic macromolecular pesticide groups to metabolites with low toxicity and poor mobility. These metabolites become further converted into secondary conjugates, transported to vacuoles, and stored in the cell wall or degraded, leading to a complete loss of toxicity [5,13]. Nevertheless, plant genetic attributes can be adopted to tackle pesticide residues effectively.

GSH performs multiple physiological activities, such as anti-oxidization, amino acid transport, detoxification, and immune response, to enhance stress defense and regulate growth and development [14]. Plants take advantage of the redox ability of GSH to protect plants from pesticide stress; GSH acts as a substrate or co-factor to combine with the pesticides and their metabolites and forms glutathione conjugates to detoxify [15]. Importantly, GSH is involved in the AsA-GSH cycle and directly reacts with H_2O_2 under the action of glutathione peroxidase (GPX) and enhances the ability of glutathione S-transferase (GST) to scavenge ROS [16,17]. *GSH2* is essential for GSH synthesis; therefore, exploring GSH function contributes to understanding the plant's molecular response to toxic compounds. Meanwhile, in rice, glutaredoxin (OsGrxs) overexpression enhanced GSH levels and reduced arsenite accumulation [18]. The *GSH2* mRNA level in sugar beet was associated with Cd concentration, and the overexpression of *GSH2* enhanced cadmium tolerance in tobacco [19,20]. Overexpression of *γ-GC* enhanced chloroacetanilide herbicide tolerance and degradation in poplar by promoting GSH accumulation and GST activity [21]. However, the biological role of *CsGSH2* in regulating propamocarb residues and phytotoxicity remains unclear.

Previously a transcriptome expression profiling of cucumber under propamocarb stress showed that the glutathione pathway played an important role in managing propamocarb residues and phytotoxicity [22]. We identified six differentially expressed genes including *Csa4M303130*, *Csa3M133380*, *Csa5M409710*, *Csa7M395820*, *Csa3M597320*, and *Csa1M571280* in the glutathione pathway under propamocarb stress. Changes in the expression of glutathione-related genes in Y3F604 (low propamocarb residues) and M729 (high propamocarb residues) showed that *Csa1M571280* (*CsGSH2*) might be a key gene in response to propamocarb stress. To further explore *CsGSH2* function, we adopted the *CsGSH2* transformation approach and analyzed the antioxidant enzyme and AsA-GSH cycle, which provided a foundation for the study of the molecular mechanism of low propamocarb residues in cucumber.

2. Materials and Methods

2.1. Plants and Treatments

Two cucumber varieties, M729 and Y3F0604, with different propamocarb residues, were used in this study; the concentration of residues in the leaves was 5.05 mg/kg in M729 and 1.95 mg/kg in Y3F0604 at 48 h after spraying propamocarb. The plants were grown at 28/18 °C (light/dark) in an incubator with a 12 h photoperiod and 70% humidity. Propamocarb (CAS:24579-73-5), obtained from Aladdin (Shanghai, China), was applied at a 2 mM concentration on the seedlings at the three-true-leaf stage (25 d after germination). All leaves were sprayed with 20 mL of propamocarb, and plants sprayed with an equivalent volume of water were maintained as the control. To determine the propamocarb content in cucumber, we collected leaves at 0.5,1, 2, 4, 6, 8, 10, 15, and 20 d after spraying propamocarb. To assess malondialdehyde (MDA) and reactive oxygen species (ROS) levels, we collected leaves at 2 d after spraying propamocarb [4]. We collected leaves at 6, 12, 24, 36, and 48 h after spraying propamocarb for qPCR analysis.

The *Arabidopsis thaliana* plants of the Columbia ecotype were grown at 22/18 °C with 16 h/8 h light/dark conditions for the transgenic experiments. The M729 genotype was used for overexpression and antisense expression in cucumber. The T_2 generation transgenic plants including OE lines (OE3, OE5, and OE7) and AS lines (AS1, AS2, and AS5) were used for analyzing *CsGSH2* function. To determine propamocarb residues between transgenic plants and the control, we collected leaves at 6, 12, 24, 36, 48, and 72 h after spraying propamocarb. To investigate antioxidant enzyme (SOD, POD, CAT, APX, DHAR, and MDHAR) activities, glutathione cycle enzyme activities (GSH, GPX, GST, and GR), and AsA-GSH content (AsA, DHA, GSH, and GSSG), we collected leaves of OE lines and AS lines at 2 d after spraying propamocarb. We collected leaves at 2 d after spraying propamocarb to measure MDA salary and ROS generation.

2.2. Determination of Propamocarb Residues

Five grams of the leaf sample were homogenized with 25 mL acetonitrile for 5 min. The supernatant was filtered and mixed with 2 g NaCl under shaking for 5 min. The sample was then placed in tubes for 30 min and concentrated using nitrogen gas blow drying at room temperature. Finally, 2 mL of acetone was added to the concentrate to analyze propamocarb residues using an Agilent 7890B-5977A gas chromatography system (Agilent Technologies, Santa Clara, CA, USA). Here, a 30 m × 0.25 mm × 0.25 μm HP-5MS capillary column was used. The oven temperature was programmed at 40 °C for 2 min, increased to 200 °C at the rate of 25 °C/min, and held for 8 min; the sample inlet was set at 240 °C in a non-split injection mode allowing a flow rate of 1.0 mL min^{-1}. The representative gas chromatogram of propamocarb is presented in Supplementary Figure S1.

2.3. Lipid Peroxidation and ROS Levels

The levels of MDA in the leaf samples were measured at 532 and 600 nm using the MDA kit (Meimian, China), following the thiobarbituric acid colorimetric method. Meanwhile, H_2O_2 and O_2^- levels were assayed using sulfuric acid peptide oxidation at 415 nm and hydroxylamine hydrochloride at 530 nm, using the corresponding kits from Solarbio (Solarbio, Beijing, China).

2.4. Real-Time Quantitative PCR

Total RNA was isolated from Y3F604 and M729 leaves using the Plant RNA rapid extraction reagent (Dining, China). Agarose gel (1%) electrophoresis and NanoPhotometer N60 (Germany) were used to examine the RNA quality and concentration. Isolated RNA was reverse transcribed into cDNA using a cDNA kit (Toyobo, Japan), and qRT-PCR was performed to analyze the gene expression patterns using the SYBR mixture (Dining, China) on an AriaMx Real-Time PCR System (Agilent Technologies, USA). The 20 μL reaction mixture contained 50 ng cDNA (2 μL), 2× Fast qPCR Master Mix (10 μL), forward primer (0.4 μL), reverse primer (0.4 μL), and DEPC water (7.2 μL). The PCR was run as follows:

94 °C for 2 min, then 40 cycles of 94 °C for 15 s, 60 °C for 30 s. Primer sequences are shown in Supplementary Table S1. The relative expression levels of the genes were calculated following the $2^{-\Delta\Delta CT}$ method [23], using the cucumber *EF1a* as an internal reference gene [24]. Three biological and four technical replicates were used for the analysis.

2.5. Subcellular Localization

The sequences of *CsGSH2*, excluding the termination codon (TAG), were amplified by PCR, and the purified PCR product was fused into the linearized pGII-eGFP at the *Hind*III and *BamH*I restriction sites by homologous recombination kit (Dining, Beijing, China). The high-purity recombinant plasmid (30 μg) and pGII-eGFP were transformed into Arabidopsis protoplasts, as reported earlier [25]. The GFP expression was captured at 16 h with light using a confocal laser scan microscope (Leica, Weztlar, Germany).

2.6. CsGSH2 Gene Construction and Transformation

The full-length CDS of *CsGSH2* was isolated from Y3F604 leaves by PCR. *GSH* sequences of cucumber, melo, pepo, durian, *Zisnnia elegans*, *Cynara cardunculus* var. scolymus, *Lupinus angustifolius*, and *Helianthus annuus* were obtained from the NCBI database and aligned using DNAMAN8.0 software. Phylogenetic analysis was performed using Mega11 software. The three-dimensional molecular structure of *CsGSH2* was determined using the SWISS-MODEL server (https://www.swissmodel.expasy.org/, accessed on 1 September 2021).

The pCAMBIA1303 vector with a CaMV35S constitutive promoter was linearized using *Bgl*II and *Spe*I restriction enzymes. Further, the purified *35S:CsGSH2* PCR product was inserted into the pCAMBIA1303 via homologous recombination (Dining, China). The recombinant plasmid was transferred into *Agrobacterium tumefaciens* LBA4404 using the freeze–thaw method and infected into Arabidopsis using floral dipping [26]. The T_3 generation transgenic plants were obtained by screening using 50 mg·L^{-1} hygromycin and confirmed using PCR and qPCR.

Furthermore, the p1250 vector with a CaMV35S constitutive promoter was linearized using the *Xcm*I restriction enzyme. The purified PCR product of *CsGSH2* was fused into the p1250 vector using a TA cloning kit (Dining, China). The forward insertion of the recombinant plasmid for the overexpression of *CsGSH2* and reverse insertion for silencing *CsGSH2* (antisense expression of *CsGSH2*) were verified using Sanger sequencing. Finally, the cotyledon nodes of M729 were infected with *A. tumefaciens* LBA4404. The T_2 generation transgenic plants were obtained by screening with 1 mg·L^{-1} L glufosinate and confirmed using PCR and qPCR [27].

2.7. Determination of Enzyme Activities and AsA-GSH Cycle

Approximately 0.1 g of the leaf sample was ground in a tube (1:10; leaf: 0.01 mol L^{-1} PH = 7.4 PBS extracting solution (*w*/*v*)), and the antioxidant enzyme activities and AsA-GSH content were measured following the micro kit instructions (Meimian Industrial Co., Ltd., Meimian, China) on an Epoch microplate reader (BioTek, Shoreline, WA, USA). The activity of SOD was assessed based on the reduction of nitro blue tetrazolium (NBT) at 560 nm [28]. The activity of POD was measured following the guaiacol method at 470 nm [29]. The CAT activity was determined based on the reduction of H_2O_2 at 240 nm [30]. The activity of APX was measured based on the rate of ascorbate (ASA) oxidation (10 and 130 s) at 290 nm [31]. The GPX activity was assayed based on the oxidation of glutathione at 412 nm [32]. Additionally, the activity of GST was determined by measuring the rate of conjugation between GSH and 1-chloro-2,4-dinitrobenzene (CDNB), and that of GR based on NADPH oxidation at 340 nm [32]. DHAR and MDHAR activities were analyzed as Sun et al. [33] described. ASA and DHA levels were determined based on the rate of AsA oxidation in 30 and 150 s and generation in 10 and 110 s, respectively, at 265 nm [34]. Leaves were washed twice with PBS, ground in liquid nitrogen, and mixed with a 10-fold extracting solution. GSH and DTNB formed a complex with a characteristic absorption peak at 412 nm, which was used to determine the GSH content [35]. Glu-

tathione disulfide (GSSG) content was determined at 412 nm following the 2-vinylpyridine method [35].

2.8. Statistical Analysis

All experiments were arranged in a randomized complete block design with three replicates (five plants in each replicate). Data are represented as mean values (±SE) of three replicates at least. Statistical analysis was performed using SPSS 18.0 (Chicago, IL, USA) software. Significant differences between the mean values were determined using Duncan's Multiple Range Test at $p < 0.05$.

3. Results

3.1. Propamocarb Stress Induces Lipid Peroxidation and ROS Accumulation in Cucumber

Our previous work showed that different genotypic varieties of cucumber differ significantly in terms of propamocarb residues [22]. An initial analysis of the propamocarb content in M729 and Y3F604 showed different amounts of residues from 2 to 20 days after propamocarb spray. The maximum residue detected in M729 was 5.07 mg/kg, and that in Y3F604 was 1.95 mg/kg. The propamocarb content decreased from 2 to 10 days. At 20 days, 1.83 and 0.46 mg/kg propamocarb residues were detected in M729 and Y3F604, respectively (Figure 1A). Compared with two cucumber genotypes in the control group, the MDA content and H_2O_2 content were not significantly different (Figure 1B,C), the O^{2-} content was higher in M729 than Y3F604 (Figure 1D). However, the MDA, H_2O_2, and O^{2-} contents were increased in two varieties under propamocarb stress. M729 showed a 40.18% increase in MDA content, while Y3F604 showed a 34.23% increase at 48 h under propamocarb stress compared with the control (Figure 1B). Additionally, H_2O_2 content increased by 41.67% in M729 and 32.28% in Y3F604 following propamocarb application (Figure 1C); the O^{2-} content increased by 44.90% in M729 and 37.95% in Y3F604 (Figure 1D). These results indicate that the stress due to propamocarb induced MDA and ROS damage in cucumber plants.

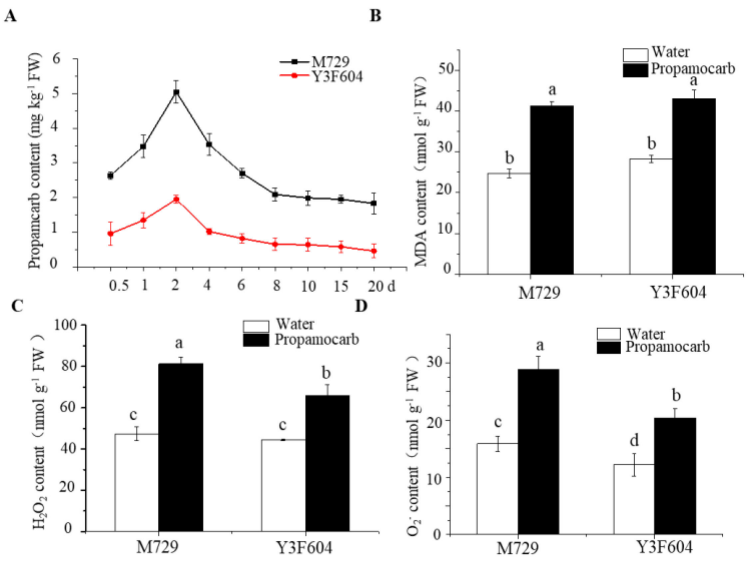

Figure 1. Propamocarb residues and phytotoxicity in the leaves of M729 and Y3F604 cucumber varieties. (**A**) Propamocarb residues at 0.5, 1, 2, 4, 6, 8, 10, 15, and 20 d; (**B**) MDA content at 2 d; (**C**) H_2O_2 content at 2 d; and (**D**) O^{2-} content at 2 d after application of 2 mM propamocarb. Data are the means of three replicates with SEs, and different letters indicate significant differences ($p < 0.05$).

3.2. CsGSH2 Regulates Glutathione Metabolism under Propamocarb Stress

Transcriptome analysis revealed genes encoding glutathione synthetase (*Csa1M571280*), glutathione-S-transferases (*Csa4M303130*, *Csa3M133380*, *Csa5M409710*, and *Csa7M395820*),

and ribonucleoside-diphosphate reductase (*Csa3M597320*) of the glutathione pathway, only *Csa1M571280* and *Csa4M303130* were differentially expressed genes ($|\log2 \text{ ratio} \geq 2|$ and FDR < 0.01) under propamocarb stress (Table 1). The qRT-PCR analysis of this study revealed that *Csa5M409710* (2.87), *Csa1M571280* (4.06), and *Csa3M597320* (2.53) were significantly upregulated in Y3F604 compared with the control, while no significant difference was observed in M729. *Csa4M303130*, *Csa7M395820*, and *Csa3M133380* were significantly upregulated in M729 and Y3F604; however, no significant difference was observed between the two cultivars, which indicates that they are generally expressed under propamocarb stress (Figure 2A). By integrating the transcriptome data and qRT-PCR results, *Csa1M571280* (*CsGSH2*) was selected as a candidate for further research.

Table 1. List of six genes of the glutathione pathway.

Gene ID	TPM/Control	TPM/Propamocarb	log2 Ratio (Propamocarb/Control)	FDR (False Discovery Rate)	Blast Annotation	Enzyme NO.
Csa4M303130	47.19	111.91	2.04	1.63×10^{-12}	Glutathione S-transferase (GST)	2.5.1.18
Csa3M133380	8.56	35.24	1.25	1.56×10^{-11}		
Csa5M409710	22.91	86.82	1.92	6.84×10^{-12}		
Csa7M395820	11.04	40.59	1.88	6.45×10^{-12}		
Csa3M597320	10.49	25.65	1.29	2.29×10^{-5}	Ribonucleoside-diphosphate reductase small chain (RDR)	1.17.4.1
Csa1M571280	2.21	13.81	2.64	5.71×10^{-6}	Glutathione synthetase (GSH)	6.3.2.2

Note: TPM: transcripts per million.

Furthermore, the analysis of the dynamic expression of *CsGSH2* in leaves showed high expression at all time points; the expression rapidly increased from 6 to 24 h and slightly decreased at 36 and 48 h in Y3F604 (Figure 2B). Meanwhile, the transcript level of *CsGSH2* was high at 12, 24, and 48 h in the leaves of M729, with no difference between propamocarb treatment and control (Figure 2C). Significantly, *CsGSH2* was upregulated at 6, 12, 24, 36, and 48 h in Y3F604 with low propamocarb residues, while there was no difference in M729 at 6, 12, 24, 36, and 48 h with high propamocarb residues, indicating that *CsGSH2* might play a crucial role in glutathione metabolism under propamocarb stress.

3.3. CsGSH2 Is a Cytosolic Protein

Arabidopsis protoplast was transfected with the *35S:CsGSH2* and *35S:GFP* plasmids to determine *CsGSH2* subcellular localization. After 16 h of light culture, the GFP fluorescent signal was detected throughout the cell due to the *35S:GFP* plasmid. Conversely, the signal was mainly detected in the cytoplasm of *Arabidopsis* cells transfected with the *35S:CsGSH2* construct (Figure 3), indicating *CsGSH2* as a cytosolic protein.

3.4. Cloning and Bioinformatic Analysis of CsGSH2

The open reading frame (ORF) of *CsGSH2* was 1650 bp, encoding 549 aa with an eu-GS domain; therefore, this protein belongs to the eu-GS superfamily (Supplementary Figure S2A). The further analysis predicted $C_{2737}H_{4341}N_{759}O_{819}S_{19}$ as the molecular formula of the protein, with a molecular mass of 61.59 kDa and an isoelectric point of 6.98. The fat index was 91.79, while the total average hydrophilicity was −0.291, which indicates that *CsGSH2* is a hydrophilic protein. Phylogenetic analysis based on GSH proteins of cucumber and other plant species revealed *CsGSH2* protein and the GSH proteins of Cucurbitaceae crops (melon and pumpkin) in the same evolutionary branch, with 90% homology (Supplementary Figure S2B). Additionally, the three-dimensional molecular structure of the *CsGSH2* protein was found to be composed of 27 β-folds (yellow) and 23 α-spirals (pink) (Supplementary Figure S2C).

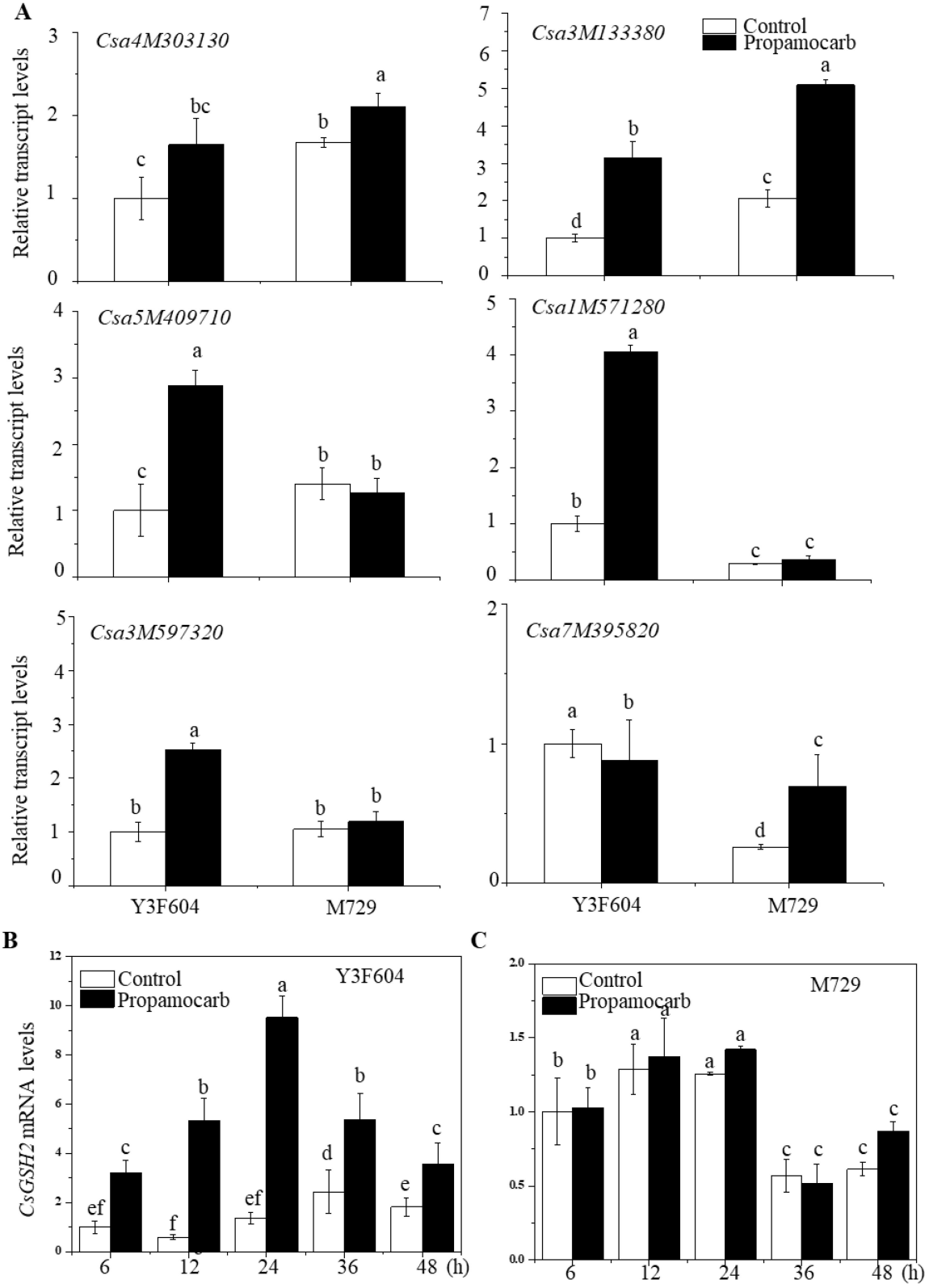

Figure 2. *CsGSH2* expression analysis in cucumber under propamocarb stress. (**A**) Expression levels of six genes of the glutathione pathway. Dynamic expression of *CsGSH2* in the leaves of (**B**) Y3F604 and (**C**) M729. The relative expression levels of the genes were analyzed by qRT-PCR using *CsEF1α* as the reference gene. Data are the means of three replicates with SEs, and different letters indicate significant differences ($p < 0.05$).

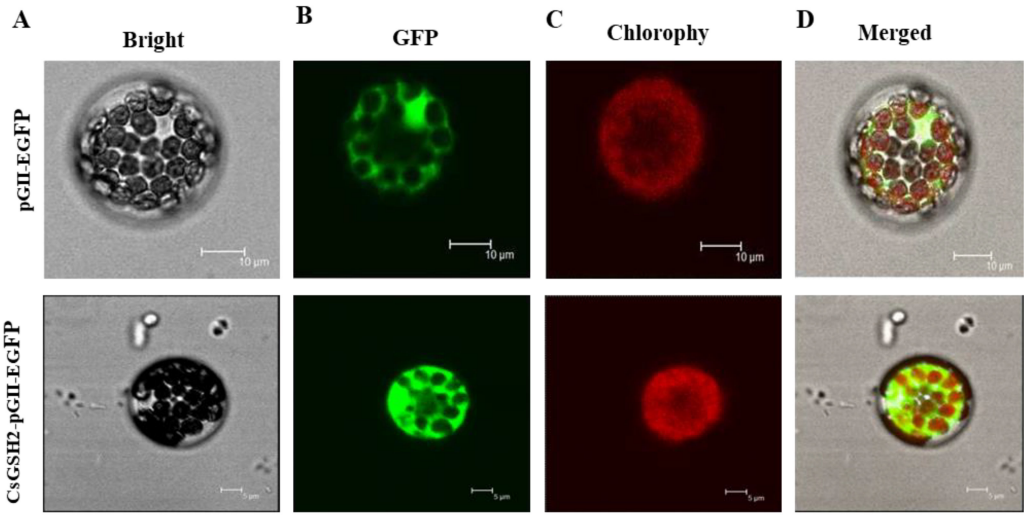

Figure 3. Subcellular localization of the *CsGSH2* protein in *Arabidopsis thaliana* protoplasts. Green fluorescence indicates the localization of the fusion protein. (**A**) Bright-field illumination. (**B**) GFP fluorescence. (**C**) Chlorophyll fluorescence. (**D**) The overlay of GFP and chlorophyll fluorescence. Bar = 10 μm.

3.5. Overexpression of CsGSH2 Alleviates Propamocarb Residues in Cucumber and Arabidopsis

The overexpression construct *CsGSH2*-p1250 (OE lines) and the antisense expression construct *CsGSH2*-p1250 (AS lines) were generated for transgenic experiments in cucumber, using the empty vector p1250 as the control. *LBA4404 Agrobacterium*-mediated infection was performed in the cotyledon nodes of M729, after differentiation culture and rooting culture, we obtained 12 transgenic plants (Figure 4). Eventually, T_2 transgenic plants, including seven OE lines, five AS lines, and two empty lines, were identified using PCR. The PCR results showed that a 1900 bp fragment contained *CsGSH2* (1650 bp) and a 250 bp fragment from the p1250 vector (Supplementary Figure S3). Three OE lines with the highest *CsGSH2* transcript expression levels (OE3, OE5, and OE7) and three AS lines with the lowest *CsGSH2* transcript expression levels (AS1, AS2, and AS5) were screened using qPCR for further analysis (Figure 5A,B). Subsequently, 2 mM of propamocarb was sprayed onto the OE lines, AS lines, and control plants with three true leaves. The analysis revealed 35.1%, 36.2%, and 32.17% lower propamocarb residues in OE3, OE5, and OE7, respectively, and 13.4%, 7.8%, and 11.9% higher residues in AS lines AS1, AS2, and AS5, respectively, compared to the control plants (Figure 5C). Further analysis revealed that the residues rapidly increased at 0–48 h and declined at 48-72 h in OE, AS, and control lines. Notably, from 6 to 72 h, the propamocarb residues in the OE line were significantly lower than those in CK, while higher than those in AS1 (Figure 5D).

These observations imply that the overexpression of *CsGSH2* alleviates propamocarb residues in cucumber. Meanwhile, the overexpression of *CsGSH2* in Arabidopsis plants enhanced the tolerance and reduction of propamocarb residues (Figure S3).

3.6. Overexpression of CsGSH2 Helps Propamocarb Detoxification

To further analyze the *CsGSH2* function, we measured GSH content in transgenic plants and controls. GSH content increased by 38.9%, 32.6%, and 35.3% in the OE3, OE5, and OE7 lines, while it decreased by 15.1%, 16.6%, and 17.1% in the AS1, AS2, and AS5 lines compared with the control plants (Figure 6A). Furthermore, the activity of the major glutathione pathway enzymes significantly increased in the *CsGSH2*-overexpressing plants. We observed a 54.2%, 36.5%, and 46.5% increase in the OE3, OE5, and OE7 plants and 33.3%, 23.7%, and 28.7% decrease in the AS1, AS2, and AS5 plants (Figure 6B). GPX and GR activities also considerably increased in the *CsGSH2*-overexpressing plants, while lower activities were detected in the antisense plants compared with the control (Figure 6C,D).

These results indicate that the overexpression of *CsGSH2* contributed to the accumulation of GSH and increased the activity of key enzymes of the glutathione pathway involved in propamocarb detoxification.

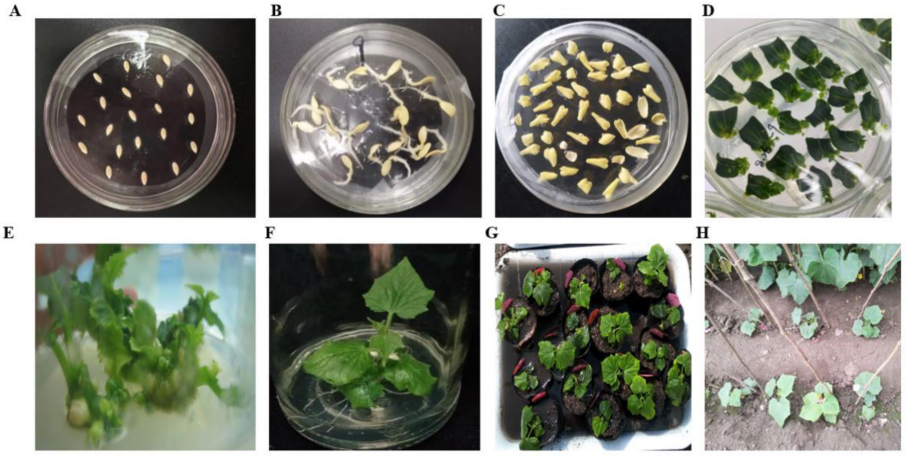

Figure 4. Genetic transformation of cucumber by *CsGSH2*-p1250. (**A**) Seeds of M729. (**B**) Seed germination. (**C**) Agrobacterium-mediated infection of cotyledon nodes. (**D**,**E**) Differentiation culture. (**F**) Rooting culture. (**G**) Domestication culture. (**H**) Transplanting in the greenhouse.

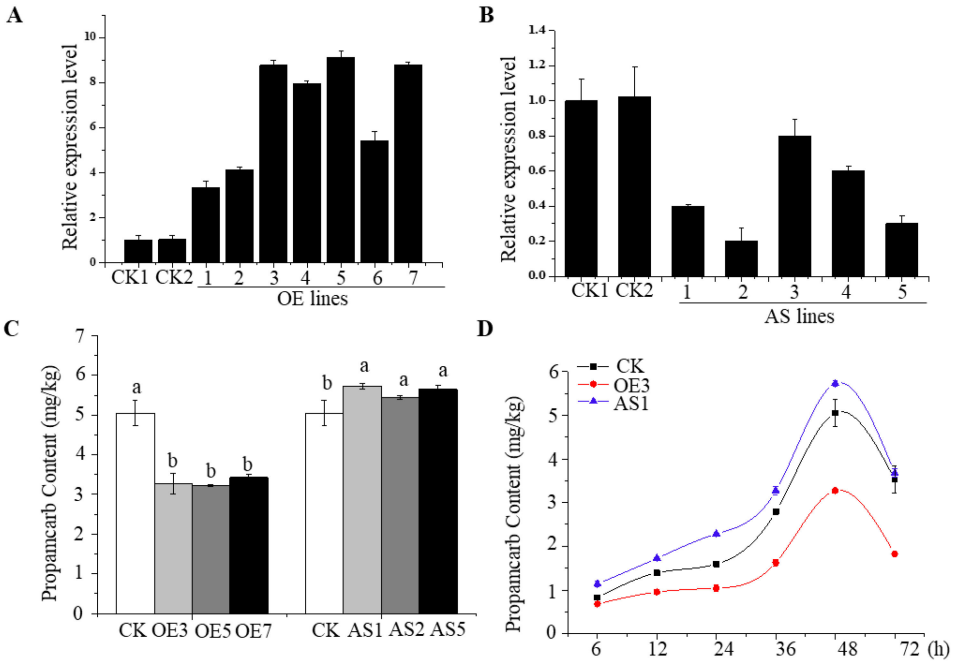

Figure 5. Effects of *CsGSH2* overexpression in cucumber. (**A**) *CsGSH2* mRNA levels in the control and *CsGSH2*-overexpressing (OX) plants. (**B**) *CsGSH2* mRNA levels in the control and antisense (AS) plants. (**C**) Propamocarb residues in the control, OX, and AS plants at 48 h after propamocarb application. (**D**) Changes in propamocarb residues in control, OX, and AS plants at 6, 12, 24, 36, 48, and 72 h after propamocarb application. Data are the means of three replicates with SEs, and different letters indicate significant differences ($p < 0.05$).

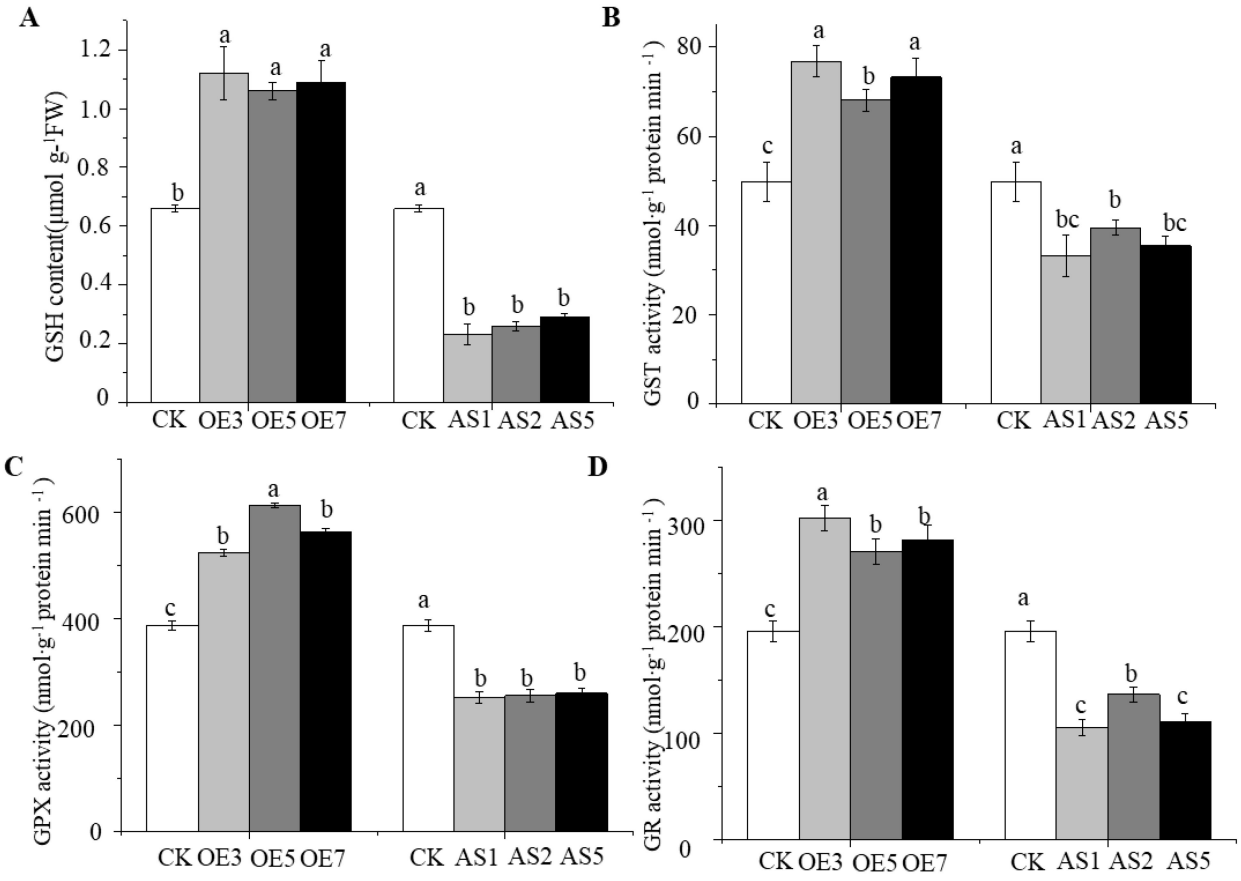

Figure 6. Content of glutathione (GSH) and activities of enzymes of the glutathione pathway in the leaves of the control, *CsGSH2*-overexpressing (OX), and antisense (AS) plants at 48 h after propamocarb application. (**A**) GSH content. (**B**) Glutathione S-transferase (GST) activity. (**C**) Glutathione peroxidase (GPX) activity. (**D**) Glutathione reductase (GR) activity. Data are the means of three replicates with SEs, and different letters indicate significant differences ($p < 0.05$).

3.7. Overexpression of CsGSH2 Enhances Antioxidant Enzyme Activities in Response to Propamocarb Phytotoxicity

Compared with the control, the OE3, OE5, and OE7 lines showed a significant increase in the activities of SOD, POD, CAT, and APX under propamocarb stress (Figure 7A–D). The POD activity was not significantly different between the antisense lines and the control plants; however, the SOD, CAT, and APX activities markedly decreased in AS1, AS2, and AS5 lines. These results collectively indicate that the overexpression of *CsGSH2* enhanced antioxidant enzyme activities in response to propamocarb phytotoxicity.

3.8. Overexpression of CsGSH2 Moderates the AsA-GSH Cycle to Reduce ROS Levels

As shown in Table 2, GSH, GSSG, and total glutathione content significantly increased in the OE3, OE5, and OE7 plants and decreased in the AS1, AS2, and AS5 plants. The GSH/GSSG ratio increased by 32%, 21%, and 26% in the OE3, OE5, and OE7 lines, respectively, and decreased by 13%, 17%, and 8% in the AS1, AS2, and AS5 plants, respectively, compared with the control. Similarly, the content of AsA and total ascorbate significantly increased in the OE3, OE5, and OE7 lines, while the content decreased in AS1, AS2, and AS5 lines. However, the DHA content was lower in the OE3, OE5, and OE7 lines than in the AS1, AS2, and AS5 lines and the control. The AsA/DHA ratio increased by 13%, 19%, and 12% in OE3, OE5, and OE7 lines, while it decreased by 18%, 10%, and 7% in AS1, AS2, and AS5 lines compared to the control; these observations indicate that the conversion of DHA to AsA was promoted in *CsGSH2*-overexpressing plants. In addition, the *CsGSH2*-

overexpressing plants demonstrated increased MDHAR and DHAR activities, while the antisense plants demonstrated decreased activities (Figure 7E–F). These results indicate that the overexpression of *CsGSH2* regulated propamocarb metabolism by moderating the AsA-GSH cycle. Furthermore, H_2O_2 and O_2^- accumulation significantly decreased in the OE3, OE5, and OE7 lines; however, the H_2O_2 content was higher in the AS lines than that in control (Figure 8A). No significant difference in the O_2^- content was observed between the AS lines and control (Figure 8B). MDA levels were consistent with the ROS levels in *CsGSH2*-overexpressing plants (Figure 8C). These results collectively indicate that the overexpression of *CsGSH2* alleviated ROS accumulation and MDA levels.

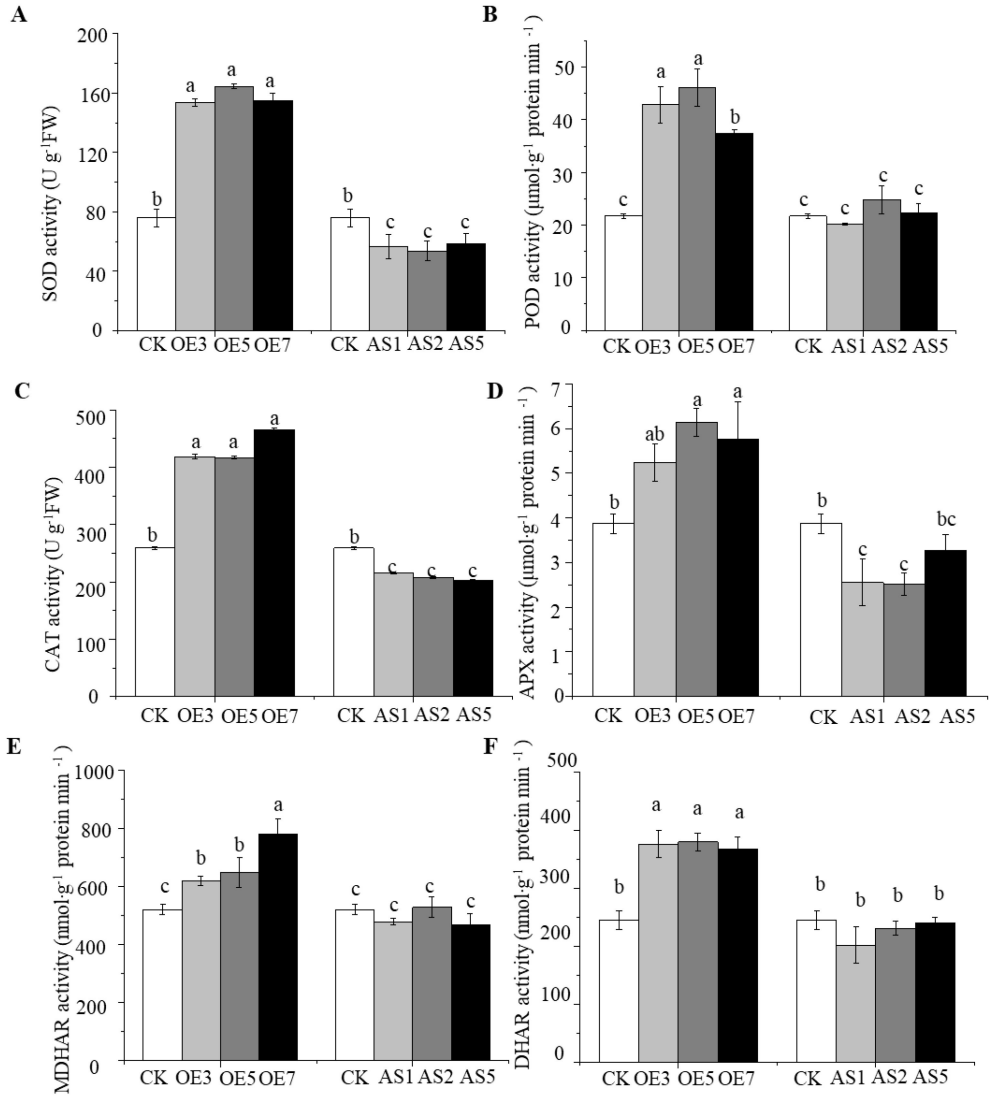

Figure 7. Antioxidant enzyme activities in the leaves of the control, *CsGSH2*-overexpressing (OX), and antisense (AS) plants at 48 h after propamocarb application. (**A**) Superoxide dismutase (SOD) activity. (**B**) Peroxidase (POD) activity. (**C**) Catalase (CAT) activity. (**D**) Ascorbate peroxidase (APX) activity. Data are the means of three replicates with SE, and different letters indicate significant differences ($p < 0.05$). (**E**) Monodehydroascorbate reductase (MDHAR) activity. (**F**) Dehydroascorbate reductase (DHAR) activity. Data are the means of three replicates with SE, and different letters indicate significant differences ($p < 0.05$).

Table 2. Ascorbate–glutathione (AsA-GSH) cycle in the leaves of control, *CsGSH2*-overexpressing (OX), and antisense (AS) plants 48 h after 2 mM propamocarb application.

Lines	AsA Content	DHA Content	Total Ascorbate	AsA/DHA	GSH Content	GSSG Content	Total Glutathione	GSH/GSSG
CK	1.42 ± 0.015 ^{b}	1.37 ± 0.031 ^{b}	2.79 ± 0.016 ^{c}	1.04 ± 0.037 ^{b}	0.66 ± 0.029 ^{b}	0.28 ± 0.009 ^{b}	0.94 ± 0.024 ^{b}	2.36 ± 0.052 ^{c}
OE3	2.21 ± 0.038 ^{a}	1.01 ± 0.019 ^{d}	3.22 ± 0.032 ^{a}	2.19 ± 0.022 ^{a}	1.08 ± 0.056 ^{a}	0.31 ± 0.015 ^{a}	1.39 ± 0.076 ^{a}	3.48 ± 0.043 ^{a}
OE5	2.34 ± 0.013 ^{a}	1.14 ± 0.021 ^{c}	3.48 ± 0.047 ^{a}	2.05 ± 0.016 ^{a}	0.98 ± 0.033 ^{a}	0.33 ± 0.007 ^{a}	1.34 ± 0.046 ^{a}	2.97 ± 0.032 ^{b}
OE7	2.15 ± 0.047 ^{a}	1.02 ± 0.027 ^{d}	3.17 ± 0.026 ^{a}	2.11 ± 0.013 ^{a}	1.02 ± 0.017 ^{a}	0.32 ± 0.010 ^{a}	1.34 ± 0.028 ^{a}	3.19 ± 0.022 ^{a}
AS1	1.02 ± 0.011 ^{c}	1.58 ± 0.020 ^{a}	2.60 ± 0.009 ^{b}	0.65 ± 0.045 ^{c}	0.37 ± 0.008 ^{c}	0.17 ± 0.004 ^{c}	0.54 ± 0.014 ^{c}	2.18 ± 0.045 ^{d}
AS2	0.92 ± 0.009 ^{c}	1.43 ± 0.015 ^{b}	2.35 ± 0.028 ^{b}	0.64 ± 0.023 ^{c}	0.39 ± 0.006 ^{c}	0.19 ± 0.011 ^{c}	0.58 ± 0.015 ^{c}	2.05 ± 0.024 ^{d}
AS5	0.97 ± 0.026 ^{c}	1.56 ± 0.008 ^{a}	2.53 ± 0.018 ^{b}	0.62 ± 0.021 ^{c}	0.41 ± 0.016 ^{c}	0.21 ± 0.012 ^{c}	0.62 ± 0.031 ^{c}	1.95 ± 0.033 ^{e}

The levels of AsA, DHA, GSH, GSSG, total ascorbate, and glutathione are presented in μmol g^{1} FW. Data are the means of three replicates with SE, and different letters indicate significant differences ($p < 0.05$).

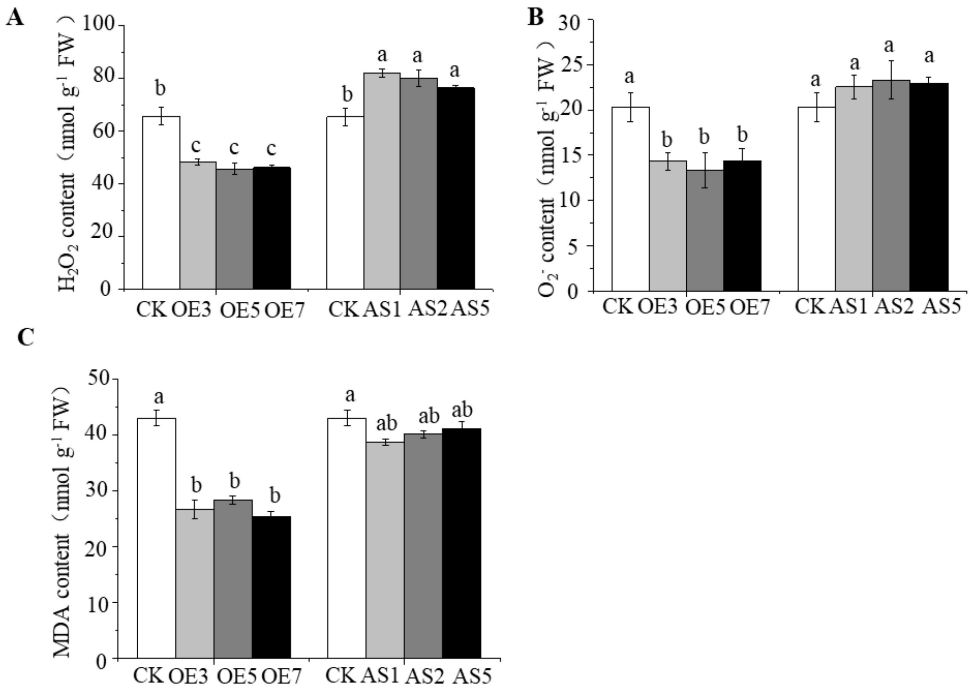

Figure 8. Reactive oxygen species (ROS) and malondialdehyde (MDA) levels in the leaves of control, *CsGSH2*-overexpressing (OX), and antisense (AS) plants at 48 h after propamocarb application. (**A**) Peroxide (H_2O_2) content. (**B**) Superoxide (O^{2-}) content. (**C**) MDA content. Data are the means of three replicates with SE, and different letters indicate significant differences ($p < 0.05$).

4. Discussion

Pesticide residues severely affect the quality of agriculture products, resulting in food insecurity, environmental pollution, and phytotoxicity [36]. Thus, how to reduce pesticide residues in crops has become a global problem and garnered research attention. Research recently showed that melatonin, brassinosteriods, cytochrome P450, glutathione, and ATP-binding cassette (ABC transporter protein) decrease herbicide and chlorothalonil residues in crops [13,37,38]. However, little has been reported about the molecular mechanisms regulating propamocarb residues in cucumber by glutathione. Propamocarb is a low-toxicity bactericide that gets absorbed internally, and it is more likely to accumulate in crops such as cucumber and result in residues above the permissible limit [39,40]. Here, we focused on the function of *CsGSH2* in detoxification via the glutathione pathway; it might be a new method of reducing propamocarb residues in cucumber.

Under propamocarb stress, the ATP-Binding cassette transporter CsABC19 was upregulated in the leaves, fruit peels, and other tissues of cucumber [41]. Furthermore, Zhang

et al. showed that mitochondrial carrier family protein *CsMCF* is involved in propamocarb stress and detected differences in expression patterns in two cucumber varieties. The mRNA abundance of the high-mobility-group protein *CsHMGB* in cucumber fruits and leaves consistently increased from 0 to 36 h and declined from 2 to 4 d under propamocarb stress [42]. Our previous study showed that propamocarb residues increased from 3 to 48 h after propamocarb application. The present study found that the propamocarb residues gradually declined from 2 to 8 d after propamocarb application. Notably, *CsGSH2* expression increased from 6 to 48 h, while propamocarb accumulation consistently increased during the first 48 h after propamocarb application. *CsGSH2* expression showed a positive correlation with *CsMCF*/*CsHMGB*/*CsABC19*, indicating a crucial role of *CsGSH2* in managing propamocarb residues and phytotoxicity. In higher plants, the cytoplasm is considered the major site of GSH synthesis [43]. In the present study, CsGSH2 protein expression was detected in the cytoplasm, indicating the significance of *CsGSH2* for GSH synthesis.

As a physiological detoxification molecule in the glutathione pathway, GSH directly regulates plants' growth and metabolic activities. GSH protected maize plants against herbicide residues and phytotoxicity by enhancing GSH accumulation and GST and P450 activities [44]. GSH also reacts with heavy metal ions or toxic substances to form a binding complex with low toxicity (GSH-X). GSH-X is then transported to the extracellular environment or metabolized by hydrolytic enzymes [45]. In *Auxenochlorella protothecoides*, GSH had chelated with Cd and balanced intracellular redox homeostasis to defend against Cd stress and toxicity [46]. In addition, GSH reacted with nitric oxide (NO) to form nitrosoglutathione (GSNO) and alleviated aluminum (Al) and Cd phytotoxicity in plants [47,48]. In the present study, overexpression of *CsGSH2* promoted low propamocarb residues in cucumber. Here, GSH might combine with propamocarb to form GSH-X for degradation and transportation. Overexpression of bacterial γ–glutamylcysteine synthetase in poplar induced higher GSH levels and GSH-dependent reactions for herbicide detoxification [21]. Exogenous application of GSH enhanced chromium (Cr^{+6}) and lead (Pb) stress tolerance, relieving heavy metal toxicity in oilseed rape and castor bean [49,50]. These earlier studies implied that GSH contributes to the metabolism and detoxification of toxic substances in plants. In the present study, overexpression of *CsGSH2* enhanced GSH accumulation. The higher GSH levels probably promoted GSH involved in propamocarb detoxification, thereby decreasing residues and phytotoxicity.

Propamocarb application might lead to two kinds of damage to cucumber, including ROS damage and phytotoxicity. Under propamocarb stress, overexpression of *CsGSH2* plants significantly decreased ROS damage by increasing the SOD, POD, CAT, and APX activities (Figure 7A–D). Additionally, ROS scavenging was effectively achieved through promoting the AsA-GSH cycle, accompanied by the total ascorbate and glutathione content under the action of DHAR and MDHAR, following with the higher ratios of AsA/DHA and GSH/GSSG (Table 2). On the basis of the role of GSH in the glutathione pathway, GSH combined with toxic substances under the action of GST to enhance plant tolerance and detoxification [51,52]. Our results showed that overexpression of *CsGSH2* decreased propamocarb residues by increasing GSH content, GR and GST activities. We conjectured that GSH might play a more important role in the glutathione pathway for propamocarb metabolism. A hypothesis model was proposed that, under propamocarb stress, the antioxidant enzymes and AsA-GSH cycle were upregulated by overexpression of *CsGSH2* for ROS scavenging. At the same time, GSH might bind to propamocarb under the action of GST to form the low-toxicity conjugates, and which are transport to the extracellular by transporters for reducing propamocarb residues and phytotoxicity in cucumber (Figure 9).

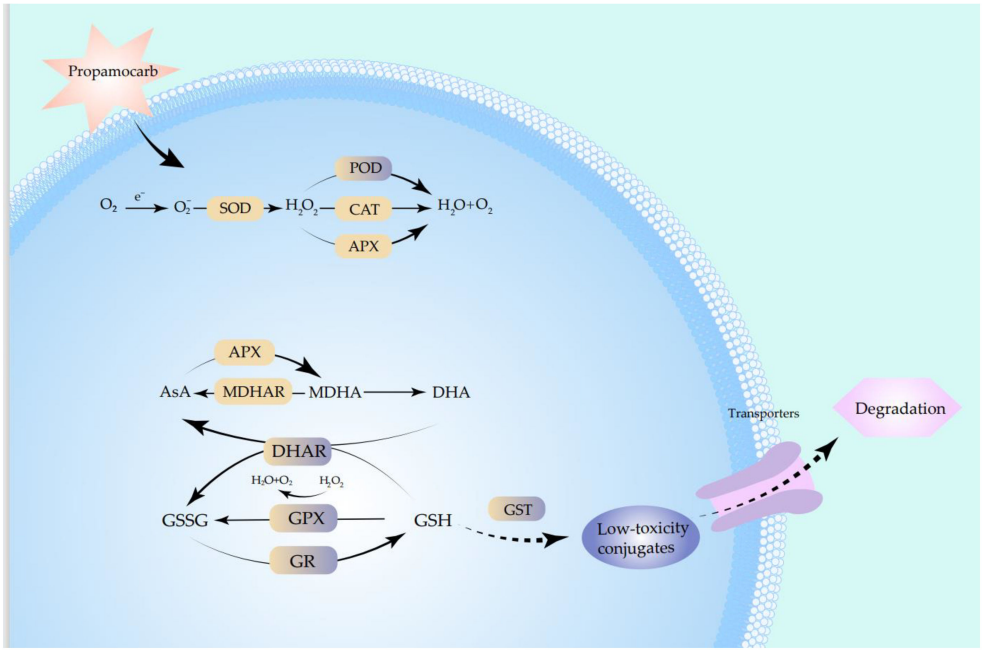

Figure 9. Hypothetical model of propamocarb metabolism and detoxification in cucumber.

GSH has strong antioxidant properties that maintain high redox potential in plants. As a nonenzymatic antioxidant, GSH is directly involved in the AsA-GSH cycle for ROS scavenging. Overexpression of *CsDIR16* and *CsMAPGE* increased SOD, POD, CAT, and GST activities and reduced ROS levels, enhancing propamocarb stress tolerance in cucumber [39,53]. The combined administration of hydrogen sulfide and silicon detoxified arsenic stress by modulating the AsA-GSH cycle and GST, GR, and DHAR activities in tomato plants [54]. In cucumber, the overexpression of *CsHMGB* alleviated propamocarb residues and phytotoxicity by promoting GST, GR, MDHAR, and DHAR activities and mRNA levels, AsA-GSH system, and antioxidant enzyme activities [4]. In the present study, GST, GR, MDHAR, DHAR activities and the AsA/DHA and GSH/GSSG ratios increased in the *CsGSH2*-overexpressing cucumber plants, which implies that the GST enzyme enhanced GSH conversion into GSSG consuming the H_2O_2 and reducing the oxidative stress induced by propamocarb.

5. Conclusions

The present study identified *CsGSH2*, a key gene of the glutathione pathway, in response to propamocarb residues and phytotoxicity. The full-length *CsGSH2* gene was 1650 bp long, and the protein was found localized in the cytoplasm. Overexpression of *CsGSH2* contributed to GSH accumulation and GST, GR, and GPX activities for propamocarb detoxification. Overexpression of *CsGSH2* regulated MDHA, DHAR, and antioxidant enzyme activities and the AsA-GSH system to reduce ROS and MDA levels under propamocarb stress. Thus, we conclude that overexpression of *CsGSH2* alleviates propamocarb residues and phytotoxicity by enhancing cucumber's antioxidant and glutathione detoxification potential.

Supplementary Materials: The following supporting information can be downloaded at: https://www.mdpi.com/article/10.3390/agriculture12101528/s1, Figure S1: The representative gas chromatogram of propamocarb; Figure S2: Cloning and bioinformatic analysis of *CsGSH2*. Figure S3: Identification of *CsGSH2*-overexpressing cucumber plants by PCR. Figure S4: Effects of *CsGSH2* overexpression in *Arabidopsis thaliana*. Table S1: Sequences of the primers used in this study.

Author Contributions: S.L. designed and conceived the research, S.L., Z.W., C.L. and L.F. performed the experiments, Y.H. and K.L. analyzed the sequencing data, S.L. wrote the entire manuscript, L.F. revised the manuscript, D.L. and G.F. edited the manuscript. All authors have read and agreed to the published version of the manuscript.

Funding: This research was funded by China Postdoctoral Science Foundation grant number 2021M701127, Natural Science Foundation of Heilongjiang Province grant number YQ2021C032 Basic Scientific Research Projects of provincial colleges and universities in Heilongjiang Province grant number 2020-KYYWF-1046.

Institutional Review Board Statement: Not application.

Data Availability Statement: All the data supporting the findings of this study are included in this manuscript and Supplementary materials.

Conflicts of Interest: There are no conflicts of interest with all authors.

References

1. Wang, Z.; Jiang, Y.; Peng, X.; Xu, S.; Zhang, H.; Gao, J.; Xi, Z. Exogenous 24-epibrassinolide regulates antioxidant and pesticide detoxification systems in grapevine after chlorothalonil treatment. *Plant Growth Regul.* **2016**, *81*, 455–466. [CrossRef]
2. Li, R.; Zhao, J.; Wu, Y.H.; Hu, F.F. Residual trend of 66.5% propamocarb hydrochloride aqueous solutions in cucumber. *J. Biosaf.* **2020**, *30*, 132–136. [CrossRef]
3. Gangemi, S.; Gofita, E.; Costa, C.; Teodoro, M.; Briguglio, G.; Nikitovic, D.; Tzanakakis, G.; Tsatsakis, A.M.; Wilks, M.F.; Spandidos, D.A.; et al. Occupational and environmental exposure to pesticides and cytokine pathways in chronic diseases. *Int. J. Mol. Med.* **2016**, *38*, 1012–1020. [CrossRef] [PubMed]
4. Li, S.N.; Xin, M.; Luan, J.; Liu, D.; Wang, C.H.; Liu, C.L.; Zhang, W.S.; Zhou, X.Y.; Qin, Z.W. Overexpression of *CsHMGB* alleviates phytotoxicity and propamocarb residues in cucumber. *Front. Plant. Sci.* **2020**, *11*, 738. [CrossRef]
5. Yin, Y.L.; Zhou, Y.; Zhou, Y.H.; Shi, K.; Zhou, J.; Yu, Y.; Yu, J.Q.; Xia, X.J. Interplay between mitogen-activated protein kinase and nitric oxide in brassinosteroid–induced pesticide metabolism in *Solanum lycopersicum*. *J. Hazard Mater.* **2016**, *316*, 221–231. [CrossRef]
6. Wang, M.; Zhang, S.; Ding, F. Melatonin mitigates chilling-induced oxidative stress and photosynthesis inhibition in tomato plants. *Antioxidants* **2020**, *9*, 218. [CrossRef]
7. Zhu, M.D.; Zhang, M.; Gao, D.J.; Zhou, K.; Tang, S.J.; Zhou, B.; Lv, Y.M. Rice *OsHSFA3* gene improves drought tolerance by modulating polyamine biosynthesis depending on abscisic acid and ros levels. *Int. J. Mol. Sci.* **2020**, *21*, 1857. [CrossRef]
8. Hou, L.Y.; Lehmann, M.; Geigenberger, P. Thioredoxin *h2* and *o1* Show Different Subcellular Localizations and Redox-Active Functions, and Are Extrachloroplastic Factors Influencing Photosynthetic Performance in Fluctuating Light. *Antioxidants* **2021**, *10*, 705. [CrossRef]
9. Hasanuzzaman, M.; Bhuyan, M.; Anee, T.I.; Parvin, K.; Fujita, M. Regulation of ascorbate-glutathione pathway in mitigating oxidative damage in plants under abiotic stress. *Antioxidants* **2019**, *8*, 384. [CrossRef]
10. Hasanuzzaman, M.; Bhuyan, M.; Zulfiqar, F.; Raza, A.; Mohsin, S.M.; Mahmud, J.A.; Fujita, M.; Fotopoulos, V. Reactive oxygen species and antioxidant defense in plants under abiotic stress: Revisiting the crucial role of a universal defense regulator. *Antioxidants* **2020**, *9*, 681. [CrossRef]
11. Guan, L.; Zhang, P.; Wang, X.K.; Ren, Y.P.; Guo, B.B.; Liu, F. Photodegradation of pyraclostrobin in water environment and microencapsulation effect on its photostability. *J. Agro. Environ. Sci.* **2015**, *34*, 1493–1497. [CrossRef]
12. Liu, N.; Li, J.; Lv, J.; Yu, J.; Xie, J.; Wu, Y.; Tang, Z. Melatonin alleviates Imidacloprid phytotoxicity to cucumber (*Cucumis sativus* L.) through modulating redox homeostasis in plants and promoting its metabolism by enhancing glutathione dependent detoxification. *Ecotoxicol. Environ. Saf.* **2021**, *217*, 112248. [CrossRef] [PubMed]
13. Zhou, Y.; Xia, X.; Yu, G.; Wang, J.; Wu, J.; Wang, M.; Yang, Y.; Shi, K.; Yu, Y.; Chen, Z. Brassino steroids play a critical role in the regulation of pesticide meta-bolism in crop plants. *Sci. Rep.* **2015**, *5*, 9018. [CrossRef] [PubMed]
14. Chin, D.C.; Hsieh, C.C.; Lin, H.Y.; Yeh, K.W. Low Glutathione Redox State Couples with a Decreased Ascorbate Redox Ratio to Accelerate Flowering in *Oncidium* Orchid. *Plant Cell Physiol.* **2016**, *57*, 423–436. [CrossRef] [PubMed]
15. Sharma, A.; Bhardwaj, R.; Kumar, V.; Thukral, A.K. Gc-Ms Studies Reveal Stimulated Pesticide Detoxification by Brassinolide Application in *Brassica juncea* L. plants. *Environ. Sci. Pollut. Res.* **2016**, *23*, 14518–14525. [CrossRef]
16. Bela, K.; Horváth, E.; Gallé, Á.; Szabados, L.; Tari, I.; Csiszár, J. Plant glutathione peroxidases: Emerging role of the antioxidant enzymes in plant development and stress responses. *J. Plant Physiol.* **2015**, *176*, 192–201. [CrossRef]
17. Kapoor, D.; Singh, S.; Kumar, V.; Romero, R.; Prasad, R.; Singh, J. Antioxidant enzymes regulation in plants in reference to reactive oxygen species (ROS) and reactive nitrogen species (RNS). *Plant Gene* **2019**, *19*, 100182. [CrossRef]
18. Verma, P.K.; Verma, S.; Meher, A.K.; Pande, V.; Mallick, S.; Bansiwal, A.K.; Tripathi, R.D.; Dhankher, O.M.; Chakrabarty, D. Overexpression of rice glutaredoxins (*OsGrxs*) significantly reduces arsenite accumulation by maintaining glutathione pool and modulating aquaporins in yeast. *Plant Physiol. Biochem.* **2016**, *106*, 208–217. [CrossRef]

19. Jia, C.C.; Ji, J.; Wang, G.; Tian, X.W.; Du, X.L.; Guan, C.F.; Jin, C.; Wu, D.Y. Over-expression of Glutathione Synthetase Gene Enhances CadmiumTolerance in Transgenic Tobacco Plant. *China Biotenol.* **2014**, *34*, 79–86. [CrossRef]
20. Liu, D.L.; Ma, L.B.; Guo, A.Y.; Yang, H.; Lu, Z.Q. Cloning of Beta vulgaris Glutathione Synthetase (*BvGS*) Gene under Cadmium Stress. *Sugar Crops. China* **2017**, *39*, 23–25. [CrossRef]
21. Gullner, G.; Kömives, T.; Rennenberg, H. Enhanced tolerance of transgenic poplar plants overexpressing γ-glutamylcysteine synthetase towards chloroacetanilide herbicides. *J. Exp. Bot.* **2001**, *52*, 971–979. [CrossRef] [PubMed]
22. Wu, P.; Qin, Z.; Zhao, W.; Zhou, X.Y.; Wu, T. Transcriptome Analysis Reveals Differentially Expressed Genes Associated with Propamocarb Response in Cucumber (*Cucumis sativus* L.) Fruit. *Acta Physiol. Plant.* **2013**, *35*, 2393–2406. [CrossRef]
23. Schmittgen, T.D.; Livak, K.J. Analyzing real-time PCR data by the comparative *C*(T) method. *Nat. Protoc.* **2008**, *3*, 1101–1108. [CrossRef] [PubMed]
24. Wan, H.; Zhao, Z.; Qian, C.; Sui, Y.; Malik, A.A.; Chen, J. Selection of appropriate reference genes for gene expression studies by quantitative real–time polymerase chain reaction in cucumber. *Anal. Biochem.* **2010**, *399*, 257–261. [CrossRef]
25. Yoo, S.D.; Cho, Y.H.; Sheen, J. *Arabidopsis* mesophyll protoplasts: A versatile cell system for transient gene expression analysis. *Nat. Protoc.* **2007**, *2*, 1565–1572. [CrossRef]
26. Bechtold, N.; Pelletier, G. In planta *Agrobacterium*-mediated transformation of adult *Arabidopsis thaliana* plants by vacuum infiltration. *Methods Molecular Biol.* **1998**, *82*, 259–266. [CrossRef]
27. Zhang, Y.; Zhang, X.; Liu, B.; Wang, W.; Liu, X. A *GAMYB* homologue *CsGAMYB1* regulates sex expression of cucumber via an ethylene independent pathway. *J. Exp. Bot.* **2014**, *65*, 3201–3213. [CrossRef]
28. Aebi, H. Catalase in vitro. *Methods Enzymol.* **1984**, *105*, 121–126. [CrossRef]
29. Bradford, M.M. A rapid and sensitive method for the quantitation of microgram quantities of protein using theprinciple of protein-dye binding. *Anal. Biochem.* **1976**, *72*, 248–254. [CrossRef]
30. Giannakoula, A.; Moustakas, M.; Syros, T.; Yupsanis, T. Aluminium stress induces up-regulation of an efficient antioxidant system in the Al-tolerant maize line but not in the Al-sensitive line. *Environ. Exp. Bot.* **2010**, *67*, 487–494. [CrossRef]
31. Durner, J.; Klessig, D.F. Inhibition of ascorbate peroxidase by salicylic acid and 2,6-dichloroisonicotinic acid, two inducers of plant defense responses. *Proc. Natl. Acad. Sci. USA* **1995**, *92*, 11312–11316. [CrossRef] [PubMed]
32. Anderson, J.V.; Davis, D.G. Abiotic stress alters transcript profiles and activity of glutathione *S*-transferase, glutathione peroxidase, and glutathione reductase in *Euphorbia esula*. *Physiol. Plant.* **2004**, *120*, 421–433. [CrossRef] [PubMed]
33. Shu, S.; Yuan, L.Y.; Guo, S.R.; Sun, J.; Yuan, Y.H. Effects of exogenous spermine on chlorophyll fluorescence, antioxidant system and ultrastructure of chloroplasts in Cucumis sativus L. under salt stress. *Plant Physiol. Biochem.* **2013**, *63*, 209–216. [CrossRef] [PubMed]
34. Law, M.Y.; Charles, S.A.; Halliwell, B. Glutathione and ascorbic acid in spinach (*Spinacia oleracea*) chloroplasts. The effect of hydrogen peroxide and of paraquat. *Biochem. J.* **1983**, *210*, 899–903. [CrossRef]
35. Anderson, J.V.; Chevone, B.I.; Hess, J.L. Seasonal variation in the antioxidant system of eastern white pine needles: Evidence for thermal dependence. *Plant Physiol.* **1992**, *98*, 501–508. [CrossRef]
36. Siddique, Z.; Malik, A.U.; Asi, M.R.; Anwar, R.; Inam Ur Raheem, M. Sonolytic-ozonation technology for sanitizing microbial contaminants and pesticide residues from spinach (*Spinacia oleracea* L.) leaves, at household level. *Environ. Sci. Pollut. Res.* **2021**, *28*, 52913–52924. [CrossRef]
37. Pan, L.; Yu, Q.; Wang, J.; Han, H.; Mao, L.; Nyporko, A.; Maguza, A.; Fan, L.J.; Bai, L.Y.; Powles, S. An ABCC-type transporter endowing glyphosate resistance in plants. *Proc. Natl. Acad. Sci. USA* **2021**, *118*, 2100136118. [CrossRef]
38. Yan, Y.; Sun, S.; Zhao, N.; Yang, W.; Shi, Q.; Gong, B. *COMT1* overexpression resulting in increased melatonin biosynthesis contributes to the alleviation of carbendazim phytotoxicity and residues in tomato plants. *Environ. Pollut.* **2019**, *252*, 51–61. [CrossRef]
39. Liu, C.; Qin, Z.; Zhou, X.; Xin, M.; Wang, C.; Liu, D.; Li, S. Expression and functional analysis of the propamocarb related gene *CsDIR16* in cucumbers. *BMC Plant Biol.* **2018**, *18*, 16. [CrossRef]
40. Wu, S.; Luo, T.; Wang, S.; Zhou, J.; Ni, Y.; Fu, Z.; Jin, Y. Chronic exposure to fungicide propamocarb induces bile acid metabolic disorder and increases trimethylamine in C57BL/6J mice. *Sci. Total Environ.* **2018**, *642*, 341–348. [CrossRef]
41. Meng, J.J.; Qin, Z.W.; Zhou, X.Y.; Xin, M. An Atp-binding cassettetransporter gene from *Cucumis sativus* L., *CsABC19*, is involved in propamocarb stress in Arabidopsis thaliana. *Plant Mol. Biol. Rep.* **2016**, *34*, 947–960. [CrossRef]
42. Zhang, F.; Xin, M.; Yu, S.Q.; Liu, D.; Zhou, X.Y.; Qin, Z.W. Expression and functional analysis of the propamocarb-related gene *CsMCF* in cucumber. *Front. Plant Sci.* **2019**, *10*, 871. [CrossRef] [PubMed]
43. Marty, L.; Bausewein, D.; Müller, C.; Bangash, S.A.K.; Moseler, A.; Schwarzländer, M.; Müller–Schüssele, S.J.; Zechmann, B.; Riondet, C.; Balk, J.; et al. Arabidopsis glutathione reductase 2 is indispensable in plastids, while mitochondrial glutathione is safeguarded by additional reduction and transport systems. *New Phytol.* **2019**, *224*, 1569–1584. [CrossRef] [PubMed]
44. Wang, Z.W.; Zhao, L.X.; Gao, S.; Leng, X.Y.; Yu, Y.; Fu, Y.; Ye, F. Quinoxaline derivatives as herbicide safeners by improving *Zea mays* tolerance. *Pestic. Biochem. Physiol.* **2021**, *179*, 104958. [CrossRef]
45. Zhang, T.; Tsutsuki, H.; Li, X.; Sawa, T. New insights into the regulatory roles of glutathione in NLRP3-inflammasome-mediated immune and inflammatory responses. *The J. Biochem.* **2022**, *171*, 367–377. [CrossRef]
46. Xing, C.; Li, J.; Lam, S.M.; Yuan, H.; Shui, G.; Yang, J. The role of glutathione-mediated triacylglycerol synthesis in the response to ultra-high cadmium stress in *Auxenochlorella protothecoides*. *J. Environ. Sci.* **2021**, *108*, 58–69. [CrossRef]

47. Sun, C.; Liu, L.; Yu, Y.; Liu, W.; Lu, L.; Jin, C.; Lin, X. Nitric oxide alleviates aluminum-induced oxidative damage through regulating the ascorbate-glutathione cycle in roots of wheat. *J. Integr. Plant Biol.* **2015**, *57*, 550–561. [CrossRef]
48. Wang, D.; Liu, Y.; Tan, X.; Liu, H.; Zeng, G.; Hu, X.; Jian, H.; Gu, Y. Effect of exogenous nitric oxide on antioxidative system and S-nitrosylation in leaves of *Boehmeria nivea* (L.) Gaud under cadmium stress. *Environ. Sci. Pollut. Res. Int.* **2015**, *22*, 3489–3497. [CrossRef]
49. Li, J.S.; Suzui, N.; Nakai, Y.; Yin, Y.G.; Ishii, S.; Fujimaki, S.; Nao, K.; Hiroki, R.; Takashi, M.; Kanna, S.L.; et al. Shoot base responds to root-applied glutathione and functions as a critical region to inhibit cadmium translocation from the roots to shoots in oilseed rape (*Brassica napus*). *Plant Sci.* **2021**, *305*, 110822. [CrossRef]
50. Zeng, F.; Mallhi, Z.I.; Khan, N.; Rizwan, M.; Ali, S.; Ahmad, A.; Hussain, A.; Alsahli, A.A.; Alyemeni, M.N. Combined citric acid and glutathione augments lead (Pb) stress tolerance and phytoremediation of castorbean through antioxidant machinery and Pb uptake. *Sustainability* **2021**, *13*, 4073. [CrossRef]
51. Ahammed, G.J.; Wang, Y.Q.; Mao, Q.; Wu, M.J.; Yan, Y.R.; Ren, J.; Wang, X.J.; Liu, A.R.; Chen, S.C. Dopamine alleviates bisphenol A-induced phytotoxicity by enhancing antioxidant and detoxification potential in cucumber. *Environ. Pollut.* **2020**, *259*, 113957. [CrossRef]
52. Li, G.Z.; Zheng, Y.X.; Chen, S.J.; Liu, J.; Wang, P.F.; Wang, Y.H.; Guo, T.C.; Kang, G.Z. TaWRKY74 participates copper tolerance through regulation of TaGST1 expression and GSH content in wheat. *Ecotoxicol. Environ. Saf.* **2021**, *221*, 112469. [CrossRef] [PubMed]
53. Zhang, F.; Qin, Z.W.; Zhou, X.Y.; Xin, M.; Li, S.N.; Luan, J. Expression and functional analysis of the propamocarb-related gene *CsMAPEG* in cucumber. *BMC Plant Biol.* **2019**, *19*, 371. [CrossRef] [PubMed]
54. Cengiz, K.; Muhammad, A. Sodium hydrosulfite together with silicon detoxifies arsenic toxicity in tomato plants by modulating the AsA-GSH cycle. *Environ. Pollut.* **2021**, *294*, 118608. [CrossRef]